INFLUENCE OF PARTIAL CURING ON RESIDUAL STRESSES AND PROCESS TIME IN ADDITIVE MANUFACTURING OF THICK THERMOSETTING COMPOSITES

F. Taddei[1,2], G. Struzziero[1] and V. Michaud[2]

[1]Laboratory for Mechanical Systems Engineering, Swiss Federal Laboratories for Materials Science and Technology (Empa), Ueberlandstrasse 129, 8600 Dübendorf, Switzerland
Email: francesco.taddei@empa.ch, Email: giacomo.struzziero@empa.ch
[2]Laboratory for Processing of Advanced Composites (LPAC), École Polytechnique Fédérale de Lausanne (EPFL), Station 12, 1015 Lausanne, Switzerland
Email: francesco.taddei@epfl.ch, Email: veronique.michaud@epfl.ch

Keywords: Additive Manufacturing, additive curing, thick composites, cure-induced defects, numerical simulation

Abstract

Thick thermosetting composites show a significant potential for high-performance applications; however, their manufacturing is still limited by the build-up of cure-induced defects, causing reduced performance or process failure. The present work investigates a concept to improve manufacturing efficiency and reliability, i.e. the additive deposition of impregnated tows while being partially cured and after they have been possibly pre-cured. This was done numerically by feeding a Finite Element Analysis (FEA) with material properties characterised as function of degree of cure and temperature, and simulating the additive deposition of a 30 mm thick laminate with a moving heat source on top. Comparing standard batch curing with additive scenarios, this study reveals that the partial curing strategy is beneficial in mitigating temperature overshoot, residual stresses, and through-thickness stress gradient during cure by up to 92%, 20% and 67%, respectively. Additionally, the total process time is decreased by 23% when depositing at 600 mm/min. However, since the thermal overshoot might be exploited to fasten the cure reaction, the optimal choice of process parameters may target the shortest process time as long as cure-induced defects are kept within acceptable levels.

1. Introduction

As the composite industry expands its applications, thick section components are increasingly employed in key industrial sectors. However, the manufacturing of thick composites poses several challenges in terms of process time and arising of process-induced defects. In the curing stage, in particular, the strong temperature spikes in the inner region of the part and the thermal gradients through thickness are source of residual stress, which might cause shape distortion, matrix microcracking, hardly predictable changes in performance, and ultimately may lead to part rejection [1,2]. All these contributions affect the manufacturing efficiency and reliability. A technique with the potential for mitigating this issue is the additive curing concept, which consists in the additive deposition of impregnated tows while being partially cured through a moving heat source and after they have been possibly pre-cured (Figure 1). Since this approach allows to deal with only a fraction of the final thickness, it might reduce cure-induced defects and process time, while preserving the mechanical performance of the final component. Moreover, it allows for eliminating the dependence of the exothermic overshoot on part thickness, making this process of great interest for the manufacturing of thick composites [3-6]. Finally, it brings alongside benefits typical of Additive Manufacturing (AM), like design flexibility, waste reduction and energy saving. The present work exploits numerical simulations to study the influence of additive curing on thermal overshoot, residual stress and process time in the manufacturing of a 100x100x30 mm carbon/epoxy laminate with cross layup. The relevant material properties to feed the Finite Element model were characterised as a function of degree of cure and temperature. A sequential thermal-

mechanical analysis in Abaqus/CAE was built using the AM plug-in and user-defined subroutines to simulate the tow deposition and the action of the moving heat source as event series, while computing the cure evolution and the generation of residual stresses. The role of the pre-cure level, deposition speed, and heat source dimensions and intensity was investigated, and the results in terms of temperature, cure degree and local stress versus time compared with those of a standard batch curing.

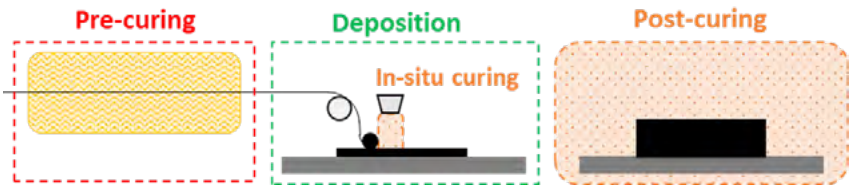

Figure 1. Schematic of the additive process with partial curing.

2. Materials and methods

2.1. Material characterisation

The resin system under investigation is composed of hot-melt epoxy resin XB3515, hardener paste Aradur® 1571 and Accelerator 1573. The thermal and mechanical properties were characterised as function of degree of cure and temperature. Differential Scanning Calorimetry (DSC) was used in isothermal (90°C, 100°C, 110°C, 120°C, 140°C), dynamic (1°C/min, 2°C/min, 10°C/min, 50°C/min) and temperature-modulated (3°C/min with amplitude of 1°C every 60 s) mode to characterise the cure kinetics and the specific heat capacity. These data were fitted by means of an autocatalytic model with explicit diffusion (Eq. 1), the DiBenedetto equation (Eq. 2), and the law for the specific heat in Eq. 3 [7,8].

$$\frac{d\alpha}{dt} = \frac{A \cdot exp(-\frac{E}{R \cdot T})}{1+exp[C(\alpha-(\alpha_C+\alpha_T \cdot T))]} \alpha^m (1-\alpha)^n \quad (1)$$

$$T_g = T_{g_0} + \frac{(Tg_\infty - Tg_0) \cdot \lambda \cdot \alpha}{1-(1-\lambda) \cdot \alpha} \quad (2)$$

$$C_p = C_{p_r} + C_{p_{rT}} \cdot T + \frac{Cp_g - Cp_r - Cp_{rT} \cdot T}{1+exp(C_c(T-Tg-\sigma-\sigma_T \cdot T))} \quad (3)$$

Where $d\alpha/dt$ is the reaction rate, α the degree of cure, T the temperature, n, m the reaction orders, A the pre-exponential Arrhenius factor, E the activation energy, C the coefficient governing the breadth of the transition, α_C the coefficient governing the chemically-controlled part of the reaction, α_T the coefficient governing the diffusion-controlled part of the reaction; Tg is the glass transition temperature, Tg_0 the glass transition temperature of the uncured resin, Tg_∞ the glass transition temperature of the fully cured resin, λ a constant governing the convexity of the non-linear regression; Cp is the resin specific heat, Cp_r and Cp_g are, respectively, the intercepts in the rubbery and glassy state, Cp_{rT} governs the temperature dependence in the rubbery state, σ, C and σ_T are the parameters governing respectively the position, breadth and temperature dependence of the material specific heat in the transition from rubber to glass.

The gel point of the resin system, which was assumed to be the cross-over point of loss and storage moduli [9], was measured by running rheological tests in oscillatory mode (0.5 Hz, 1 Hz) at isothermal conditions (100°C, 110°C, 120°C). The storage modulus of the resin (E_{resin}) was characterised through Dynamic Mechanical-Thermal Analysis (DMTA) tensile tests on partially cured neat resin specimens (60x10x4 mm) at oscillation frequency of 1 Hz and heating rate of 3°C/min from 0°C to 220°C, and it was modelled using Eq. 4 [10,11].

$$E_{resin} = E_{rub} + \frac{Eglass - Eglass_T \cdot T - Erub}{1 + exp(C_m(T - Tg - \sigma_m))} \quad (4)$$

Where E_{rub} is the modulus at the rubbery state, E_{glass} and E_{glassT} control the behaviour at the glassy state with respect to temperature, σ_m and C_m govern, respectively, the position and breadth of the modulus in the transition from rubber to glass.

The coefficient of thermal expansion (CTE) was measured by utilising Distributed Fibre Optic Sensors (DFOS) that exploit the naturally-occurring Rayleigh backscatter in the glass fibre. The optical fibres were embedded in neat resin plates during casting; then, the material was partially cured and cut in specimens with approximate length 95-102 mm, width 20-30 mm and thickness 4 mm (Figure 2). All the specimens were tested in the temperature range 20-200°C with a heating rate of 1°C/min. At the same time, another sensor was inserted in a PTFE tube to be used as compensation for the thermal expansion of the glass and the effect of temperature on its optical properties. The experimental results for the CTE of the resin (a_{resin}) were fitted and modelled with Eq. 5 [10].

Figure 2. Setup for resin CTE measurement via DFOS.

$$a_{resin} = a_{rub} + a_{rub\alpha} \cdot \alpha + \frac{a_{glass} - a_{rub} - a_{rub\alpha} \cdot \alpha}{1 + exp(C_{CTE}(T - Tg - \sigma_{CTE}))} \quad (5)$$

Where a_{rub} and a_{glass} are the CTE values of the uncured polymer at the rubbery and glassy state, $a_{rub\alpha}$ controls the rubbery state with respect to the degree of cure, σ_{CTE} and C_{CTE} are the parameters governing, respectively, the position and breadth of the resin CTE in the transition from rubber to glass.
The shrinkage, thermal conductivity and the Poisson's ratio of the matrix were taken from literature and supplier datasheets, as well as the properties of the carbon fibres (Saertex U-C-298g/m2-1270mm) [8,10,12,13].

2.2. Finite Element Analysis

A sequential model in Abaqus/CAE was developed and linked to user-defined subroutines. Each simulation was run twice, where the first run was a thermal analysis (element type DC3D8), and the second run was a static analysis (element type C3D8). The thermal analysis computed the temperature field by solving the energy balance equation between the heat provided, the reaction heat and the heat dissipated by convection and/or conduction. Such temperature field was, then, imported into the static analysis, which calculated the degree of cure and the stress field by using the mechanics of anisotropic materials [3,10]. This required the implementation of the following user-defined subroutines:

- UMATHT for thermal properties, cure kinetics model and energy balance [14].
- UMAT for thermo-mechanical properties, cure kinetics, stiffness matrix of transversely isotropic linear elastic materials and strain tensors of anisotropic materials [1,15,16].
- SDVINI for the initial conditions.
- DISP for the cure cycle on the mould side.

- FILM for the convective boundary conditions.

The properties of the composite were obtained from the properties of the reinforcement and the matrix through the rule of mixtures with a fibre volume fraction of 0.55. The modelled geometry was a square-based 100x100 mm laminate made of 15 layers of 2 mm each (total thickness 30 mm) with cross layup. Each layer was meshed with 3 elements in the thickness direction, for a total of 112500 elements. The progressive activation of the elements to mimic the material deposition and the action of the moving heat source were implemented by adapting the Abaqus plugin "AM Modeler" [17], which operates with three main input data types:

- Event series to define the time, space (coordinates) and amplitude of the occurrence of the events, in particular the material deposition and the motion of the heat source.
- Parameter table to provide all the parameters needed to define the material deposition (type of activation, type and size of the bead, stack direction etc.) and the moving heat source (type of energy distribution, size and subdivision of the heat box, etc.)
- Property table to set parameters that depend on temperature or other fields, like the heat absorption coefficient.

In this study, the activation of the elements was performed as depicted in Figure 3. The movement of the heat source, which was defined as a uniform energy distribution in a rectangular parallelepiped with a square base, followed the same path. The absorption coefficient was set to the constant value of 0.88. Regarding the boundary conditions, a fixed temperature (80°C) was defined on the mould side, a deposition temperature of 80°C was given to the newly deposited elements, and natural convection (coefficient 13 W/(m^2*K)) at room temperature (25°C) was applied anywhere else (Figure 3). Once the deposition stage was concluded, the post-curing stage was simulated by defining the prescribed cure cycle (60 min dwell at 120°C) as a fixed temperature on the mould side and a convection condition on the other surfaces with coefficient equal to 50 W/(m^2*K). The simulated scenarios were decided by varying four parameters: printing speed (300 mm/min, 600 mm/min), heat source box sides (20 mm, 30 mm), energy intensity level (1, 2), and pre-cure level (2%, 20%, 40%). The reference scenario of standard batch manufacturing was simulated with a cure stage according to the Manufacturer Recommended Cure Cycle (60 min at 120°C and 120 min at 140°C). Heating and cooling ramps were defined at 1°C/min.

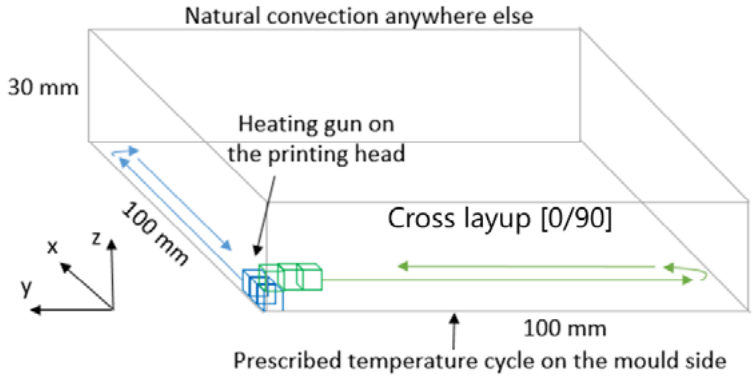

Figure 3. Model built in the FEA software: geometry, boundary conditions, material deposition path.

3. Results and discussion

3.1. Material characterisation

The results from the experiments and the phenomenological models of the storage modulus and the CTE are plotted in Figure 4 and Figure 5, while the fitting parameters of all models are reported in Table 1. The behaviour of the modulus (Figure 4) during transition reflects the state change of the material according to its level of partial cure, the speed of the reaction and the temperature [10,18]. The ascending region in the 77%-cured sample occurs because the glass transition temperature increases faster than the

test temperature; after the peak, the resin resumes transitioning to rubbery because the reaction decelerates, as cure completion approaches, while the test temperature constantly increases. The CTE (Figure 5) shows a slight increase with temperature up to the glass transition region, where the resin softens and the strain transfer to the sensor is less efficient. Moreover, the partially cured samples undergo curing and, consequently, shrink. Both contributions explain the drop of the CTE. When the reaction is completed, the CTE curves tends to align to higher values. For data fitting, average constant values are computed at the lowest and highest temperatures, whereas the transition is modelled as a smooth step. The gelation of the matrix system under investigation is estimated at an averaged degree of cure of 0.59±0.02.

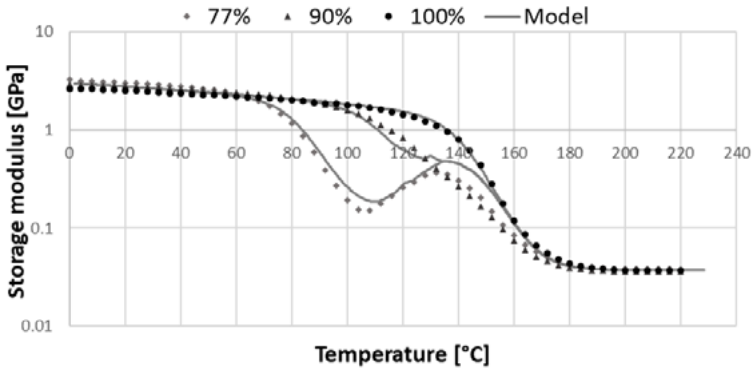

Figure 4. Fitting of experimental data of the storage modulus of partially cured resin samples from DMTA.

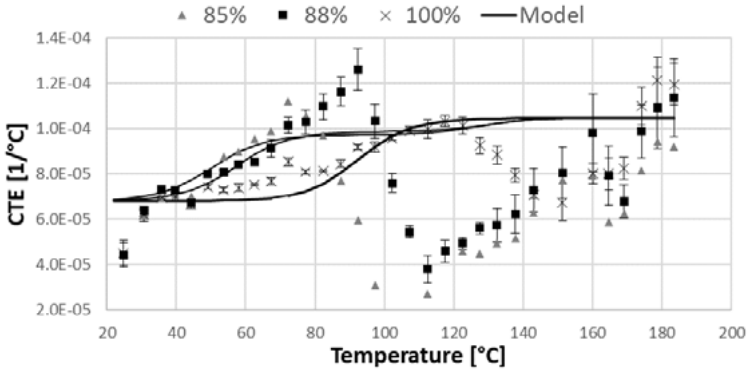

Figure 5. Fitting of experimental data of the CTE in partially cured resin samples from DFOS strain measurements.

Table 1. Fitting parameters of the models describing the resin properties.

Parameter	Value	Unit	Parameter	Value	Unit
n	1.49	/	T_{g0}	2	°C
m	0.68	/	$T_{g\infty}$	140	°C
A	4.04E+10	s^{-1}	λ	0.40	/
E	97236	J mol^{-1}	E_{rub}	3.71E+7	Pa
C	28.65	/	E_{glass}	3.01E+9	Pa
α_c	-1.0739	/	E_{glassT}	11.75E+6	Pa $°C^{-1}$
α_T	5E-3	K^{-1}	C_m	0.14	$°C^{-1}$
Cp_r	1.6014	J g^{-1} K^{-1}	σ_m	2.26	°C
Cp_{rT}	0.00249	J g^{-1} K^{-2}	a_{glass}	6.8E-5	$°C^{-1}$

Cp_g	1.5135	J g^{-1} K^{-1}	a_{rub}	5.6E-5	$°C^{-1}$
C_c	0.15	K^{-1}	$a_{rub\alpha}$	4.9E-5	$°C^{-1}$
σ	29.64	K	C_{CTE}	0.13	$°C^{-1}$
σ_T	-0.21	/	σ_{CTE}	-47.5	°C

3.2. AM simulations

The main results from the AM simulations, taken from a central element of the 9th layer, are summarised in Figure 6, which shows the temperature overshoot and stress gradient through thickness in the scenarios with printing speed 600 mm/min and heat source size 0.02 m, and Figure 7, reporting the temperature overshoot and longitudinal residual stress from all simulations against the partial degree of cure after the deposition stage. The exothermic overshoot was computed as the difference between the maximum material temperature and the prescribed cure temperature at the same instant of time. The stresses are negative because of the chemical shrinkage of the resin, the thermal compression during the cooldown, and the negative coefficient of thermal expansion of the carbon fibres. For the same printing speed and heat source dimension, the thermal overshoot and residual stress gradient between the 9th layer and 15th layer generated in the post-curing stage are reduced by up to 90% and 37%, respectively, when the energy intensity in the deposition stage and the pre-cure level are higher (see Figure 6). This means that the crucial parameter is the partial cure level reached at the end of the deposition stage and before the post-curing stage. This is represented in Figure 7 where the degree of cure after deposition is plotted against the temperature overshoot and residual longitudinal stress during post-curing, independently of pre-cure level, printing speed and heat source parameters used to reach that degree of cure. By comparing the scenario of standard curing (MRCC, 0.02 cure degree) with the scenario of highest degree of cure after deposition (0.67), the exothermic overshoot, the residual stress (in absolute value), and the through-thickness stress gradient are reduced by up to 92%, 20%, and 67%, respectively. Moreover, the total process time when printing at 600 mm/min is 23% lower than the standard curing case. However, comparing the different AM scenarios with same printing speed, it was observed that the material reaches the full cure state slightly earlier when it is pre-cured less. This is due to the effect of the temperature overshoot, which can play a role in speeding up the cure. Optimal design choice could, therefore, involve exploiting the overshoot from the reaction to cure the material faster as long as it is below values that would cause unacceptable defects.

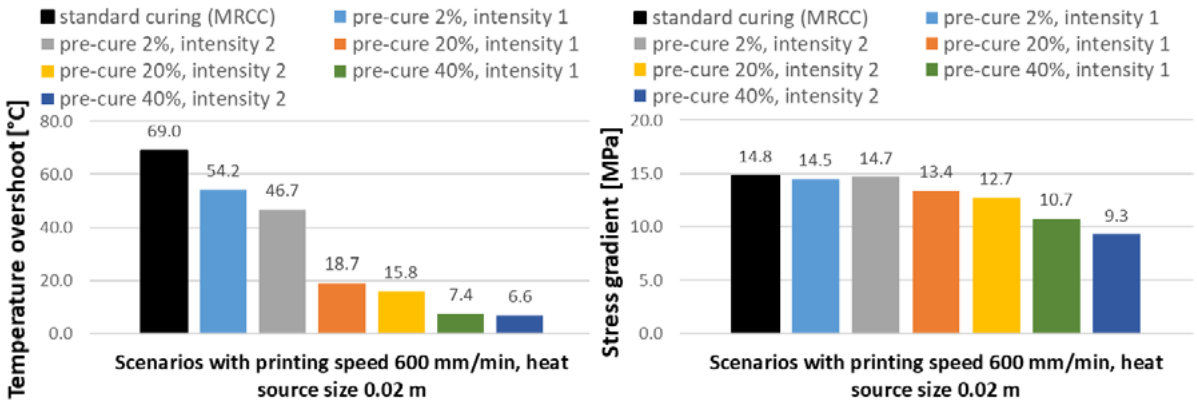

Figure 6. Temperature overshoot and through-thickness stress gradient from numerical simulations of standard curing and AM at 600 mm/min with partial curing.

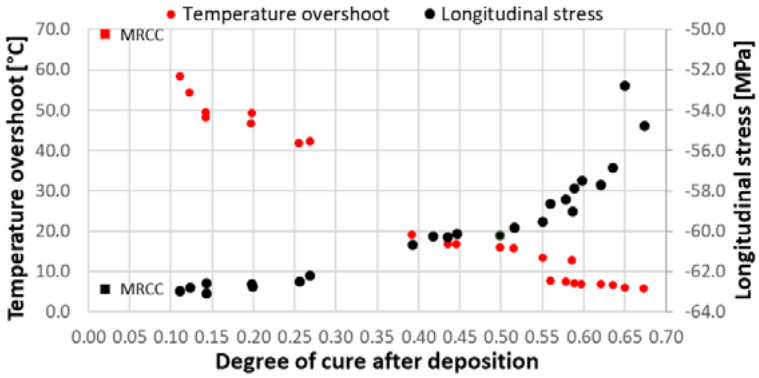

Figure 7. Role of the degree of cure after the deposition stage on the temperature overshoot and the residual longitudinal stress generated during post-curing.

4. Conclusions

The present study addressed, through numerical simulations, the potential benefits in terms of cure-induced defects and process time of a AM approach for thick thermosetting composites involving additive curing. It was found out that the main parameter affecting the temperature overshoot and residual stress generation during post-curing was the degree of partial cure reached at the end of the deposition stage. In particular, a level of partial curing during deposition up to 0.67 can reduce the temperature overshoot by up to 92%, the residual stress by up to 20%, and the stress gradient through-the-thickness by up to 67% compared to the standard batch curing using the MRCC. Furthermore, by depositing additively the material at 600 mm/min, the total process time can be decreased by 23%. However, it was observed that the stronger thermal spike in the scenarios with a lower level of partial cure contributed to fasten the cure process and, therefore, shorten the process time. This means that the optimal choice of process parameters might be a compromise between a faster manufacturing and the need to keep the thermal overshoot within acceptable levels that would guarantee the required part quality and performance. Future studies should investigate the limits in the degree of partial cure at the deposition stage since the viscosity of the polymer should not exceed values that would prevent a good adhesion between the tows and would limit the resin flow capability to fill gaps and voids during consolidation.

Acknowledgments
This work was supported by the Laboratory for Mechanical Systems Engineering, Swiss Federal Laboratories for Materials Science and technology (Empa) through the Empa Board of Directors.

References

[1] T. A. Bogetti and J. W. Gillespie. Process induced stress and deformation in thick section thermoset composite laminates. *Journal of Composite Materials*, 26(5):626-660, 1992.
[2] B. Wang, S. Fan, J. Chen, W. Yang, W. Liu and Y. Li. A review on prediction and control of curing process-induced deformation of continuous fiber-reinforced thermosetting composite structures. *Composites Part A: Applied Science and Manufacturing*, 165:107321, 2023.
[3] G. Struzziero, M. Barbezat and A. A. Skordos. Assessment of the benefits of 3D printing of advanced thermosetting composites using process simulation and numerical optimisation. *Additive Manufacturing*, 63:103417, 2023.
[4] F. Taddei, M. Barbezat, G. Struzziero and E. Troiani. Influence of pre-curing stage in additive manufacturing of advanced thermosetting composites. In *European Conference on Composite Materials (ECCM20)*, pages 385-392, 2022.
[5] A. A. Skordos and J. Kratz. Layer-by-layer curing (LbL) - Feasibility study final report. 2018.

[6] S. R. White and C. Kim. A simultaneous lay-up and in situ cure process for thick composites. *Journal of Reinforced Plastics and Composites*, 12(5):520-535, 1993.
[7] P. I. Karkanas and I. K. Partridge. Cure modeling and monitoring of epoxy/amine resin systems. I. Cure kinetics modelling. *Journal of Applied Polymer Science*, 77(7):1419-1431, 2000.
[8] G. Struzziero, B. Remy and A. A. Skordos. Measurement of thermal conductivity of epoxy resins during cure. *Journal of Applied Polymer Science*, 136(5):47015, 2019.
[9] M. Zarrelli, A. A. Skordos and I. Partridge. Investigation of cure induced shrinkage in unreinforced epoxy resin. *Plastics, Rubber and Composites*, 31:377-384, 2002.
[10] G. Struzziero, G. M. Maistros, J. Hartley and A. A. Skordos. Materials modelling and process simulation of the pultrusion of curved parts. *Composites Part A: Applied Science and Manufacturing*, 144:106328, 2021.
[11] M. Sadeghinia, K. M. B. Jansen and L. J. Ernst. Characterization and modeling the thermo-mechanical cure-dependent properties of epoxy molding compound. *International Journal of Adhesion and Adhesives*, 32:82-88, 2012.
[12] T. J. Vaughan and C. T. McCarthy. Micromechanical modelling of the transverse damage behaviour in fibre reinforced composites. *Composites Science and Technology*, 71(3):388-396, 2011.
[13] G. Struzziero and J. J. E. Teuwen. A fully coupled thermo-mechanical analysis for the minimisation of spring-in and process time in ultra-thick components for wind turbine blades. *Composites Part A: Applied Science and Manufacturing*, 139:106105, 2020.
[14] X. Yan. Finite element modeling of curing of epoxy matrix composites. *Journal of Applied Polymer Science*, 103(4):2310-2319, 2007.
[15] O. G. Kravchenko, S. G. Kravchenko and R. B. Pipes. Cure history dependence of residual deformation in a thermosetting laminate. *Composites Part A: Applied Science and Manufacturing*, 99:186-197, 2017.
[16] J. Skrzypek and A. Ganczarski. *Mechanics of Anisotropic Materials*. Springer, 2015.
[17] N. An, G. Y. Yang, K. Yang, J. Wang, M. E. Li and J. X. Zhou. Implementation of Abaqus user subroutines and plugin for thermal analysis of powder-bed electron-beam-melting additive manufacturing process. *Materials Today Communications*, 27, 2021.
[18] I. Baran, R. Akkerman and J. H. Hattel. Material characterization of a polyester resin system for the pultrusion process. *Composites Part B: Engineering*, 64:194-201, 2014.